Journal of Physics: Conference Series

PAPER • **OPEN ACCESS**

Effects of Sweep on the Flutter of Wraparound Fins

To cite this article: E Demir *et al* 2023 *J. Phys.: Conf. Ser.* **2526** 012110

View the article online for updates and enhancements.

You may also like

- Effect of petroleum hydrocarbons on the carbon and nitrogen stable isotope composition of *Nitzschia closterium*
Na Li, Yu Liu, Zhengyu Liang et al.
- Magnetic-flutter-induced pedestal plasma transport
J.D. Callen, C.C. Hegna and A.J. Cole
- An emerging impact of Eurasian spring snow cover on summer rainfall in Eastern China
Taotao Zhang, Tao Wang, Yingying Feng et al.

This content was downloaded from IP address 144.122.201.61 on 11/09/2023 at 17:17

Effects of Sweep on the Flutter of Wraparound Fins

E Demir[1,2], H L Şahin[1,3], V Z Doğan[2] and Y Yaman[3]

[1] Roketsan Missiles Inc., Ankara, Türkiye
[2] Istanbul Technical University, Istanbul, Türkiye
[3]Middle East Technical University, Ankara, Türkiye

Corresponding authors: demr.elif7@gmail.com, harunleventsahin@gmail.com

Abstract. In the field of missile and rocket design, efficiency is a crucial aspect considering factors such as weight, storage, stealth, and cost. Wraparound fins (WAFs) have been used for many years to control the trajectory of missiles and rockets because of their compactness and effectiveness. However, WAFs are structurally more flexible than other types of fins, which may negatively impact their dynamic behavior and aeroelastic response. This can cause catastrophic instabilities, such as flutter. To mitigate these challenges, it is essential to consider both aerodynamic and structural models of WAFs during the design process. In this study, the flutter velocity and frequency of WAFs were investigated in relation to different structural design configurations and sweep angles, in order to understand and improve the aeroelastic performance of swept WAFs.

1. Introduction

Tube-launch arrangements are often preferred for missiles in order to meet storage, transportation, and deployment requirements. Since the 1970s, WAFs have been used specifically in tube-launched or dispenser-launched missiles/sub-munitions. The wraparound configuration allows the fins to be folded neatly around the body, particularly in a cylindrical shape, and deployed after exiting the tube to provide aerodynamic stability. This configuration conserves valuable space and enables more missiles or larger missiles to be packaged in the tube [1].

However, the cylindrical shape of the WAF can also compromise the dynamic stability of the projectile. The asymmetry of the WAF geometry and changes in the rolling moment coefficient with Mach number are the main reasons for this dynamic instability [2]. Therefore, the curved fin configuration will affect the solution of the aeroelastic flutter problem differently.

Research on the aeroelastic flutter problem of WAFs is relatively limited. Many scholars have used a standard WAF projectile, designed by the Technical Cooperation Program (TTCP), as a baseline configuration for their numerical and experimental investigations. Although this configuration is commonly used, the WAF geometry of the TTCP standard projectile is too stiff to investigate the flutter problem. With today's technology allowing for more flexible and lightweight designs than the TTCP standard projectile, this research has selected a different fin geometry, which is more prone to the flutter problem, as the baseline geometry.

Content from this work may be used under the terms of the Creative Commons Attribution 3.0 licence. Any further distribution of this work must maintain attribution to the author(s) and the title of the work, journal citation and DOI.
Published under licence by IOP Publishing Ltd

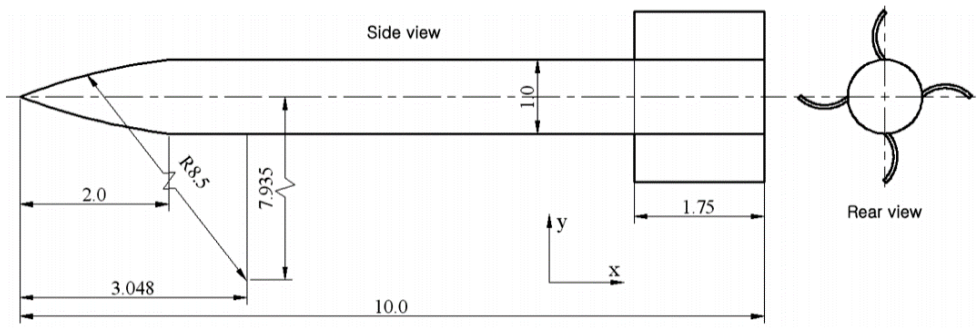


Figure 1. Overall geometry for the TTCP standard configuration [3].

Paek and his colleagues have conducted a series of studies to determine the influence of rolling effects on the aeroelastic stabilities of WAFs [4]. They calculated the roll moment coefficients and studied the roll reversal phenomenon for projectiles with WAFs (TTCP standard configuration). Later, Paek and Lee investigated the aeroelastic effects on the roll characteristics of the same projectile configuration [5]. This study was the first attempt to understand the aeroelastic roll characteristics of WAFs in the literature. In 2002, Paek et al. examined the aeroelastic stabilities of WAFs in rolling motion, in the supersonic flow region, where the fins are subjected to both aerodynamic and centrifugal forces [6]. A similar study was conducted by Kim et al. in 2012 [3], in which they also studied the flutter characteristics of a rolling WAF projectile, again the TTCP standard configuration, considering aeroelastic deflections in supersonic flow regimes. Na et al. investigated the nonlinear aeroelastic characteristics of a rolling WAF, a swept fin configuration, with free-play nonlinearity [7]. Rivera, Jr. conducted experimental and analytical studies in the Langley Transonic Dynamic Tunnel to investigate the effects of span-wise curvature on the flutter characteristics of cantilever wings for the first time [8]. Rivera, Jr. selected a generic wing geometry shown in Figure 2, which is named as Langley Research Center (LRC) configuration in this study.

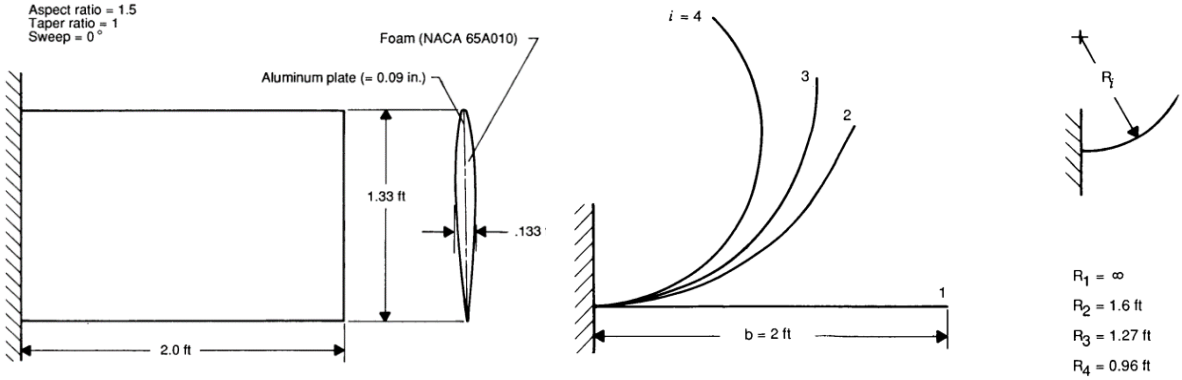


Figure 2. The geometric properties of the LRC configuration [8].

In the literature, most studies have focused on the effects of roll-rate on flutter results. However, there are not enough parametric studies of WAFs for aeroelastic performance. This study is designed to comprehensively investigate the effects of sweep angle on the aeroelastic behavior of WAFs. In this study, first, to validate the developed mathematical model, frequency and flutter analyses are conducted, and the results are compared with Rivera's experimental study [8]. The LRC configuration is used as the baseline geometry since it is more flexible than the TTCP configuration. The subsonic flow field is chosen to eliminate the roll-rate and reversal effects. Secondly, the effect of a one-step sweep angle on the aeroelastic performance of WAFs is investigated by cropping the LRC curved fin configuration with different angles. Finally, the effects of two-step sweep angle on the WAFs are investigated using the Design of Experiment (DOE) method.

2. Methods and Validation Study

In this section, Rivera's [8] experimental studies are utilized to validate numerical results for the span-wise curved fin, and a comparison of the results is presented.

The dimensions of the LRC rectangular fin in SI units can be summarized as follows: Fin span is 609.4 mm, chord length is 405.384 mm, aspect ratio of the fin is 1.5 and the fin thickness is 2.295 mm. The curved fin configuration is just a bent version of the rectangular fin geometry, which has the same chord length. Moreover, the material of the fin is taken as aluminum for the analyses. Material properties are: The Young's modulus is 68.9 GPa, the Poisson's ratio is 0.3 and the density of the material is 2860.0 kg/m^3.

2.1. Comparison of natural frequencies.

Natural frequencies and mode shapes of the curved fin are determined by using the commercial finite element analysis software Abaqus Standard®. Finite element model of the curved fin is created by using 96 eight-node shell elements (S8R). Since the experiments were conducted on a cantilever fin, fixed boundary conditions are imposed to the root of the fin along the chord. The damping effects are neglected in the frequency analysis. The natural frequencies and the mode shapes of the first four modes are shown in Figure 3.

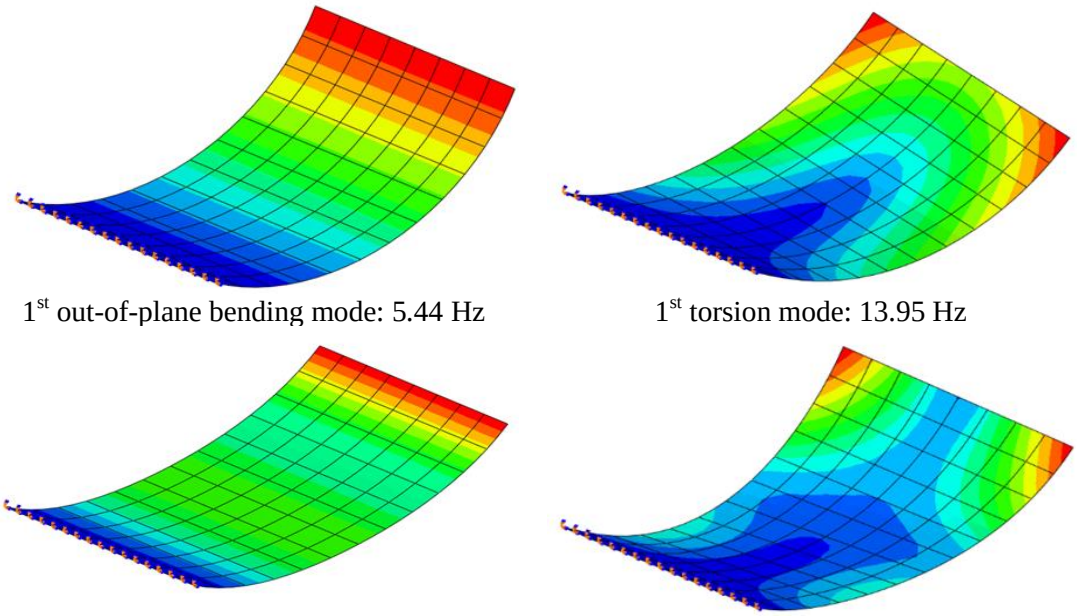


Figure 3. The first four natural frequencies and the mode shapes of the curved fin.

The natural frequencies obtained from the numerical analysis using Abaqus Standard software are compared to the experimental results of the reference study [8] to validate the accuracy of the developed mathematical model. The comparison is shown in Table 1, and it can be seen that the developed model agrees well with the experimental results.

Table 1. Comparison of the natural frequencies.

Mode	[8] [Hz]	Present Study [Hz]	Error [%] wrt [8]
1	5.4	5.44	0.82
2	14.1	13.95	-1.04
3	26.0	26.25	0.98
4	39.6	38.27	-3.35

2.2. Comparison of flutter results.

ZAERO® software was used for numerical analysis of flutter. The software requires input of eigenvalues and eigenvectors obtained from the frequency analysis. To connect the Finite Element Analysis (FEA) model and aerodynamic surfaces, the Thin Plate Spline (TPS) method is applied to the aeroelastic model with a suitable aerodynamic box number.

Flutter outputs are obtained by g-method, which utilizes the damping perturbation method. The flutter velocity, frequency and dynamic pressure are investigated in the subsonic flow regime.

The results obtained from the developed method are compared with those from the experimental study [8] in Table 2. The numerical results for the velocity and dynamic pressure are in good agreement with experimental results. However, there is a discrepancy in the flutter frequency, which is believed to be caused by neglecting the damping effects of the experimental conditions as previously mentioned.

Table 2. Comparison of the flutter outputs.

Flutter Output	[8]	Present Study	Error [%] wrt [8]
Velocity, V_f [m/s]	106.3	105.4	-0.84
Frequency, f_f [Hz]	9.8	11.1	13.20
Dynamic pressure, q_f [Pa]	2380.0	2371.0	-0.37

3. Parametric Investigation of the Sweep Angle

In this section, results from the investigation on the effects of one and two-step sweep angles on a curved fin configuration are presented.

3.1. One-step sweep angle.

As shown in Figure 4, the impact of a one-step sweep angle on the aeroelastic performance of a curved fin was examined by altering the angles of the reference curved fin to 10°, 15°, 20°, 25°, 30°, 35°, and 40°. The fin geometry with a one-step sweep angle is illustrated in Figure 4.

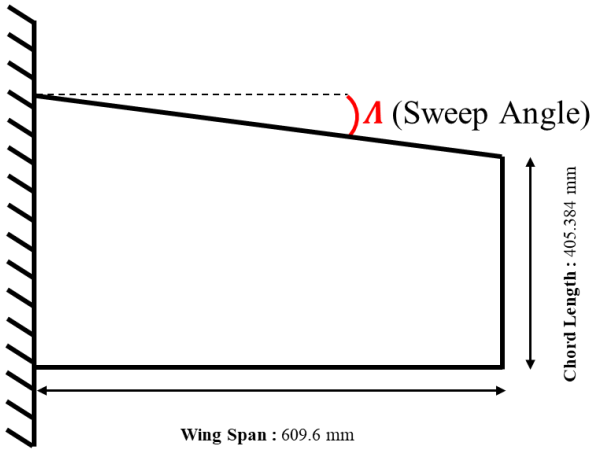


Figure 4. Dimensions of the curved swept fin.

Variations of the normalized flutter velocity and normalized flutter frequency with respect to the sweep angle Λ, are presented in Figure 5. In this graph, $V_{f_{baseline}}$ is the flutter velocity of the baseline geometry and $f_{f_{baseline}}$ is the flutter frequency of the baseline geometry. The reference values presented in Table 2 have been used to normalize all of the outputs shown in Figure 5.

The normalized flutter velocity follows a similar trend to studies found in literature [11], [12], where it exhibits a non-linear trend with the sweep angle as depicted in Figure 5. The normalized flutter

velocity initially decreases with an increasing sweep angle up to 15°, then increases until 40°. On the other hand, the normalized flutter frequency continuously increases with the sweep angle, as expected. This can be observed in Figure 6, where the ratio of the bending/torsional stiffness to the mass also increases, though the trend is not linear. In Figure 6, $\omega_{b_{baseline}}$ represents the first out-of-plane bending frequency of the baseline geometry, and $\omega_{t_{baseline}}$ represents the first torsional frequency of the baseline geometry.

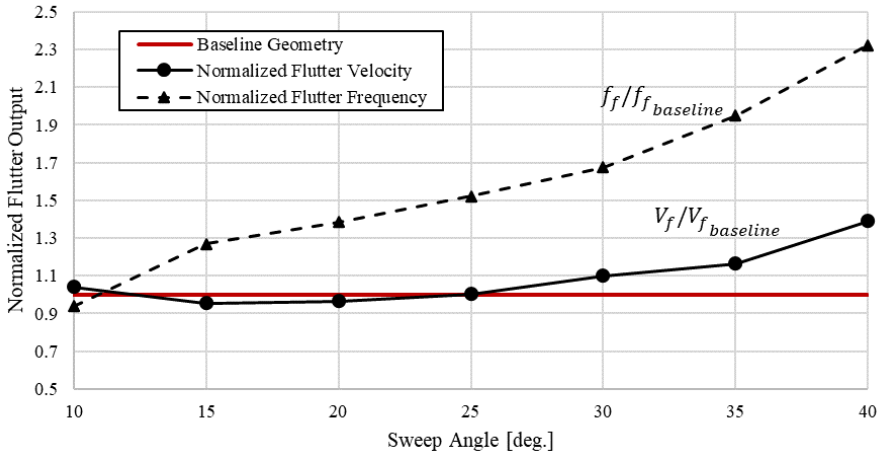


Figure 5. Normalized flutter velocity and normalized flutter frequency with respect to the sweep angle.

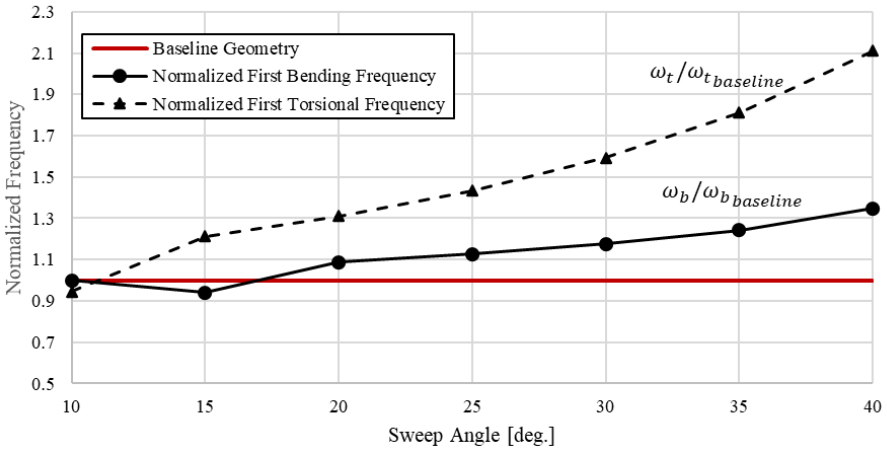


Figure 6. Normalized natural frequencies with respect to the sweep angle.

3.2. Two-step sweep angle.

In this section, the effects of two-step sweep angle on the aeroelastic behavior of curved fins are investigated using the Design of Experiment (DOE). The design parameters of the DOE include the first sweep angle, Λ_1, second sweep angle, Λ_2, and the starting position of the second sweep angle, which is labeled as the station number. These parameters are illustrated in Figure 7.

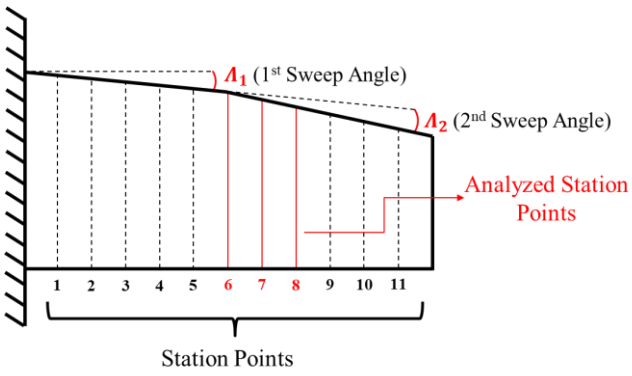


Figure 7. Representation of the curved two-step swept fin.

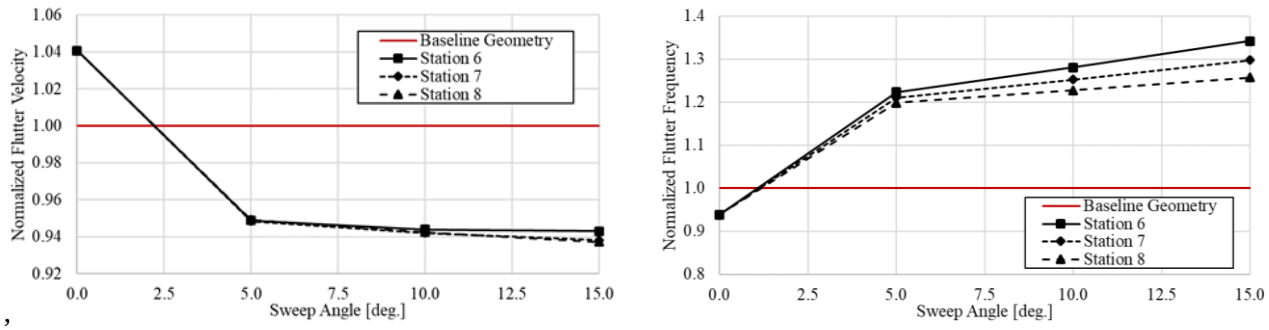
In Figure 7, the fin span is divided into twelve equidistant strip lines and the position of the strip lines starting from the fin root are labeled as the station number. In order not to decrease the lifting surface area and change the aerodynamic characteristic of the fin, the second sweep angle is assumed to start from the station numbers 6, 7 and 8 only. All DOE parameters are given in Table 3.

Table 3. Parameters of the DOE.

Λ_1 [deg.]	Λ_2 [deg.]	Station Point
10	5	6
20	10	7
30	15	8

The DOE consists of 3 cases. In each case, Λ_1 has been assigned values of 10, 20, and 30 degrees, respectively. In all cases, Λ_2 varied between 5 to 15 degrees with increments of 5 degrees. Each case is repeated for the stations 6, 7, and 8. Therefore, a total of 27 experiments are conducted.

3.2.1. In the case of the first sweep angle is 10°. In the case of $\Lambda_1 = 10°$, the normalized flutter velocity and the normalized flutter frequency with respect to Λ_2 and the station number has been illustrated in Figure 8. As seen from the graph, while the flutter frequency increases with the addition of a second sweep angle to the fin, the increase of Λ_2 and the station number has negative impacts on the flutter velocity when compared to the baseline flutter velocity. In other words, the addition of a second sweep angle to a first sweep angle of $\Lambda_1 = 10°$ results in a performance that is inferior to that of a one-step sweep angle.



(a) **(b)**

Figure 8. (a) Normalized flutter velocity with respect to second sweep angle, **(b)** Normalized flutter frequency with respect to second sweep angle.

3.2.2. In the case of the first sweep angle is 20°. In Figure 9, the effects of adding a second sweep angle to a first sweep angle of $\Lambda_1 = 20°$ on the normalized flutter velocity and normalized flutter frequency are presented. The results show that, in contrast to the previous case, the flutter velocity has an increasing trend, but the slope of the normalized flutter velocity changes depending on the station point where the second sweep angle is started. The addition of a second sweep angle from station number 8 does not have a significant effect on the flutter velocity. When comparing the results, the maximum performance is observed at station number 6 with a second sweep angle of $\Lambda_2 = 15°$, which is the only case that is favorable compared to the baseline flutter velocity for a first sweep angle of 20 degrees.

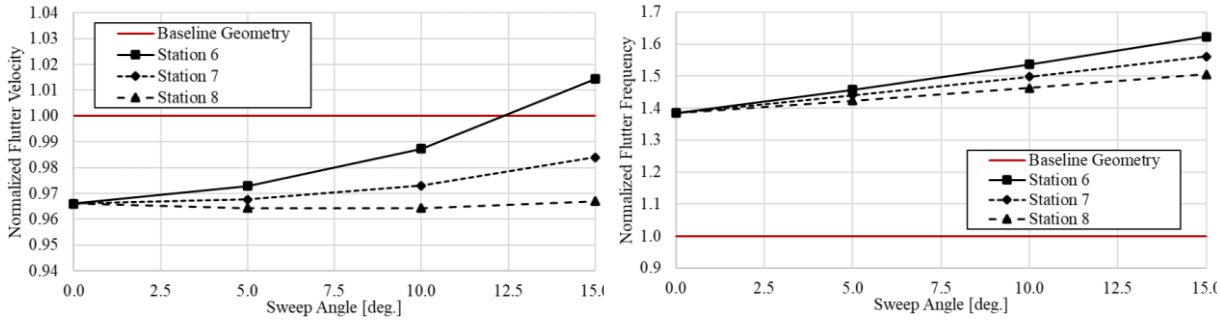


Figure 9. (a) Normalized flutter velocity with respect to second sweep angle, **(b)** Normalized flutter frequency with respect to second sweep angle.

3.2.3. In the case of the first sweep angle is 30°. In Figure 10, the effects of adding a second sweep angle to a fin with an initial angle of 30° are shown. The graph demonstrates the changes in normalized flutter velocity and normalized flutter frequency as the second sweep angle is increased. The results indicate that regardless of where the second angle starts, the fin exhibits improved flutter performance. This is evident from the increase in both normalized flutter velocity and normalized flutter frequency. Similar to the case with an initial angle of 20°, the maximum increase in normalized flutter velocity is observed at station number 6 with a second angle of 15°. The outcomes of the third case are consistent with those of the second case.

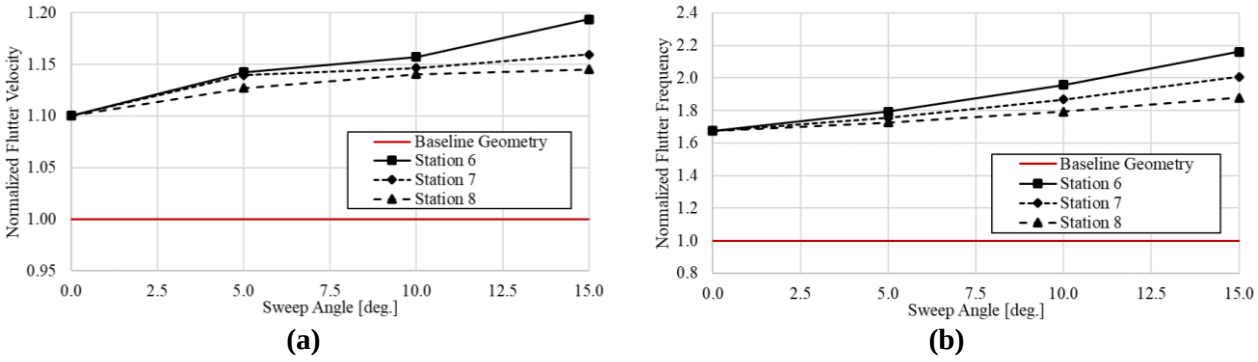


Figure 10. (a) Normalized flutter velocity with respect to second sweep angle, **(b)** Normalized flutter frequency with respect to second sweep angle.

4. Conclusions

In this study, the effect of sweep angle on the aeroelastic behavior of wraparound fins (WAFs) was extensively investigated. The validity of the finite element and aerodynamic models was confirmed using a previously published study [8]. The effect of a one-step sweep angle on the aeroelastic performance of WAFs was then studied. The results showed that the addition of a one-step sweep angle on WAFs is not always beneficial in terms of non-dimensional flutter velocity, as the trend is nonlinear. The normalized flutter velocity decreases when a sweep angle is initially added, but after 15°, it starts to increase with increasing sweep angle. On the other hand, the normalized flutter frequency continuously increases with the sweep angle due to an increasing ratio of the first out-of-plane bending frequency of the fin to the first torsion frequency.

Next, the effects of a two-step sweep angle were explored by varying multiple design parameters. The results of the two-step sweep angle showed that the normalized flutter velocity has a nonlinear trend and the normalized flutter frequency continuously increases with the addition of the second sweep angle. In all experiments, the first group of the design of experiments (DOE) had a lower non-dimensional flutter velocity compared to the unswept fin. However, in the second group, only one result ($\Lambda_2 = 15°$ at station 6) was higher than the unswept fin's velocity. All variations in the third group improved the flutter velocity compared to the non-swept fin and its one-step swept counterparts.

Although fins with sweep angles greater than 30° have good dynamic aeroelastic performance, they may not produce the required torque to control the missile/rocket due to a reduced lifting surface area. As a result, finding the optimum sweep angle value is a multidisciplinary task, where designers must increase the planform area while also considering the aeroelastic performance.

References

[1] Winchenbach G L, Buff R S, Whyte R H and Hathaway W H 1986 Subsonic and transonic aerodynamics of a wraparound fin configuration *J. Guid.* **9** 6 627-632 doi: 0.2514/3.20156
[2] Edge H L 1994 Computation of the roll moment for a projectile with wrap-around fins *J. Spacecr. Rockets* **31** 4 615-620 doi: 10.2514/3.26486
[3] Kim J Y, Cho S I and Lee I 2012 Flutter characteristics of a rolling wraparound fin projectile considering aeroelastic deflections *J. Spacecr. Rockets* **49** 4 709-719 doi: 10.2514/1.A32164
[4] Paek S K, Park T S, Bae J S, Lee I and Kwon H 1999 Computation of roll moment for projectile with wraparound fins using euler equation *J. Spacecr. Rockets* **36** 1 53-58 doi: 10.2514/2.3432
[5] Paek S K and Lee I 1999 Aeroelastic effects on the roll characteristics of a wraparound fin projectile *J. Spacecr. Rockets* **36** 4 524-530 doi: 10.2514/3.27195
[6] Paek S K, Bae J S and Lee I 2002 Flutter analysis of a wraparound fin projectile considering rolling motion *J. Spacecr. Rockets* **39** 1 66-72 doi: 10.2514/2.3783
[7] Na H J, Kim C G, Lee I, Kim J Y and Bae S B 2017 Nonlinear aeroelastic analysis of a rolling wraparound fin *J. Spacecr. Rockets* **54** 5 1041-1049 doi: 10.2514/1.A33516
[8] Rivera Jr J A 1989 Experimental and analytical investigation of the effect of spanwise curvature on wing flutter at mach number of 0.7 *NASA Tech. Memo. 4094* NASA Langley Research Center 505-63-21-02 Hampton VA 23665-5225
[9] Abaqus/Standard 6.14-5 2014 *Dassault Systemes*
[10] ZAERO 2019 *ZONA Technology Inc.*
[11] Barmby J G, Cunningham H J and Garrick I E 1951 Study of effects of sweep on the flutter of cantilever wings *Rep. 1014* National Advisory Committee for Aeronautics
[12] Ertürk B and Yaman Y 2019 Assessment of the performance of a cruise missile wing depending on design parameters at various flight conditions *MATEC Web Conf.* **304** 02009 1-8 doi: 10.1051/matecconf/201930402009